Three-dimensional Cellular Automata for Reaction-Diffusion Systems

Jörg R. Weimar
Institute of Scientific Computing,
Technical University Braunschweig
D–38092 Braunschweig, Germany
Tel. +49-531-391-3006; E-mail J.Weimar@tu-bs.de

Abstract

Cellular automata for reaction-diffusion systems are efficient enough to make the simulation of large three-dimensional systems feasible. The principal construction mechanisms used here are not much different from those for two-dimensional cellular automata. Diffusion is realized through a local averageing, and all the nonlinear reaction terms are collected in a table-lookup. The special issue in three dimensions is the need to increase time- and space-scales as much as possible to achieve sufficient system sizes. This can be done through the use of numerical integration schemes for constructing the lookup table, and through the use of special diffusion operators. We present examples of complex three-dimensional behaviours in an excitable reaction-diffusion system and in a model of a pattern-forming chemical reaction.

1 Introduction

Nonlinear reaction-diffusion systems arise in many different contexts. Examples include the spreading of infectious diseases (e.g., rabies in foxes) or of ideas and innovations, the propagation of neural signals or excitation signals in the heart muscle, the proliferation of bacterial populations, and of course chemical reactions. Some of these systems are naturally two-dimensional, but many are also naturally three-dimensional. The difficulty in simulating these nonlinear reaction-diffusion (R-D) systems comes from the fact that in many cases changes in the state (chemical composition) take place everywhere at a high rate. For simulation methods, this means that both the spatial and the temporal resolution must be high. Especially in three dimensions, this leads to a very large number of degrees of freedom.

In this paper we discuss a method of simulating three-dimensional R-D systems by cellular automata (CA). The method is based on previous work on two-dimensional CA [8, 9, 11]. The special advantage of the method is that the amount of storage needed for each cell is very small, that the time-step can be very large, and that the simulation is efficient independently of the complexity of the nonlinearity in the R-D system. The disadvantage is that fairly detailed knowledge about the phase space of the system must be aquired.

2 Reaction-Diffusion Systems

Reaction-diffusion systems are described by a set of partial differential equations of the form

$$\dot{x}_i = D_i \nabla^2 x_i + f_i(x_1, x_2, \cdots, x_s) \quad (i = 1, \cdots, s) \tag{1}$$

Usually the functions f_i are highly nonlinear, as are the solutions to the systems we are interested in.

As examples we use first the Fitz-Hugh-Nagumo model [2, 6]

$$\frac{\partial u}{\partial t} = D_u \nabla^2 u + (a-u)(u-1)u - v \tag{2a}$$

$$\frac{\partial v}{\partial t} = e(bu - v) \tag{2b}$$

with (somewhat arbitrary) parameters $a = 0.1$, $e = 0.005$, $b = 1.0$. This is an example for excitable media, which show complex behaviours such as travelling waves. In three dimensions these travelling waves can form complex organizing centers depending on the exact way different wavefronts meet. Such complex three-dimensional phenomena are important in the analysis of some heart diseases where three-dimensional rotating waves prevent the ordinary beating of the heart [13, 14].

A second example models a real reaction-diffusion system, namely the CIMA (chloride-iodide-malonic acid) reaction, in which Turing patterns were first observed in the laboratory [7, 1]. The complex reaction mechanism is simplified to a system of two equations [5]:

$$\dot{u} = D_u \nabla^2 u + A - u - \frac{uv}{1+u^2} \tag{3a}$$

$$\dot{v} = D_v \nabla^2 v + 4Bu - B\frac{uv}{1+u^2}. \tag{3b}$$

This model allows Turing patterns for some parameter values as long as $D_v > D_u$. We use $D_v = 9D_u$, which is within the experimental range. For values of $A > 6.455$ and small values of B, the system oscillates. For intermediate values of B, Turing structures appear, and for large values of B, the steady state is stable. Here we use $A = 30$ and $B = 17$, which leads to the formation of tripes in one dimensional systems, hexgonal spot spattern in two dimensions, and complex tubes in three dimensions.

3 Cellular Automata

The cellular automata we use to simulate these R-D systems are closely related to explicit finite difference schemes, and also related to coupled map lattices [4]. As in finite difference schmes, space is discretized in regular cells and time is discretized in regular time steps. In each time step the new state of all cells is calculated based on the state of the cells at the previous time step. More explicitly, the new state of a cell depends only on a finite number of neighboring cells. Thus the CA is related to the explicit schemes and cannot reach the stability properties of implicit numerical schemes.

In distinction to finite difference schemes and coupled map lattices, in the CA also the state of each cell is discretized. This means that the different variables of the R-D system are not represented by real variables (or their usual approximation, floating-point numbers), but by small integers. Often it is sufficient to select a discretization that uses numbers so small that all the variables of the R-D system, usually at least two or three, can be represented in one machine integer of 32 bits.

The total updating step can be considered to consist of three substeps. First, a sum of local neighbors is calculated, which approximates the diffusion operator. Then, the nonlinear reaction terms are added, and finally a roundoff operator is applied.

The three steps are

$$\tilde{x}(t, \mathbf{r}) = \sum_{\mathbf{r}^* \in \mathcal{N}} a(\mathbf{r}^*) x(t, \mathbf{r} + \mathbf{r}^*) \tag{4a}$$

$$\tilde{\tilde{x}}(t,\mathbf{r}) = \tfrac{1}{c}\big(\tilde{x}(t,\mathbf{r}) + c\Delta t\, f(\tilde{x}(t,\mathbf{r}))\big) \quad (4b)$$

$$x(t+\Delta t,\mathbf{r}) = R\left[\tilde{\tilde{x}}(t,\mathbf{r})\right]. \quad (4c)$$

Here $\mathcal{N}$ is the neighborhood, e.g., $\mathcal{N} = (0,0,0),(\pm 1,0,0),(0,\pm 1,0),(0,0,\pm 1)$ for the seven point Laplacian, and apart from a scaling factor c, $a(\mathbf{r}^*)$ are the coefficients for the Laplacian, usually $\frac{a(\mathbf{r}^*)}{c} = 1/7$. The introduction of the scaling factor c is useful to make all coefficients $a(\mathbf{r}^*)$ have integer values (here $c = 7$ and $a(\mathbf{r}^*) = 1$). This means that $\tilde{x}(t,\mathbf{r})$ is also discrete and can be stored in an integer. In fact, when several variables are packed into one integer, it is possible to calculate the local sum for all of them at once if they use the same diffusion coefficient. Stability of the diffusion operation is assured when none of the weights $a(\mathbf{r}^*)$ is negative (for the small operators this is equivalent to the CFL condition).

The second operation introduces the nonlinear function $f(\tilde{x})$ multiplied by the time step Δt, which leads to values that are definitely not discretized any more. Therefore the rounding operator R is needed to convert the values back to discrete values. For the rounding operator there are many possibilities, which are discussed in detail in [9, 10]. The most useful options are to round deterministically to the next discrete value, to round probabilistically, or to use a deterministic rounding that spreads the roundoff error to other values close by in phase space. Deterministic rounding can be used when the number of states is sufficiently high (usually at least 200), and it has been ascertained that no spurious effects appear. Probabilistic rounding is more time-consuming, but assures that on average, the rounding does not introduce a bias.

In the cellular automaton, the second and third step is implemented as a table lookup. Since the result of the first operation is a vector of integer values with a finite range, it is possible to calculate the result of the second and third operation once for each possible outcome of the first operation. This outcome can then be stored in a table, and at runtime only the sum has to be calculated, and a table-lookup performed. This makes the simulation time independent of the complexity of the nonlinear functions f_i, since they are only evaluated for the construction of the table and not used in the simulation.

In three dimensions it is especially important that the spatial scale be as large as possible, and that not too many neighbors be involved in the calculation of the diffusion operation. There are three possible neighborhoods that come to mind. First, use a cube of size $3 \times 3 \times 3$ centered around the cell to be updated. This smallest cube contains already 27 cells. The second possibility is to use only the nearest neighbors. This leads to the usual seven-point star. A third possibility is to use operator splitting and in one step only involve the two nearest neighbors in one dimension, and in subsequent steps use the other dimensions. Figure 1 shows these possibilities.

In this figure, the value $\tilde{D}$ is used. This value gives the intrinsic diffusivity of the operator used. It relates the time- and space-scales with the diffusion coefficient of the R-D system:

$$\frac{\Delta t}{\Delta r^2} D_i = \tilde{D}_i. \quad (5)$$

The selection of a diffusion operator with a small value of $\tilde{D}$ means that we increase Δr for a given Δt. But how can we increase the time step Δt?

The time step Δt is limited by the nonlinear reaction term f. Let us ignore for a moment the spatial dependence and the rounding. The differential equation we want to solve is

$$\dot{x} = f(x). \quad (6)$$

Using the Euler method, we approximate this by

$$x(t+\Delta t) = x(t) + \Delta t\ f(x(t)). \quad (7)$$

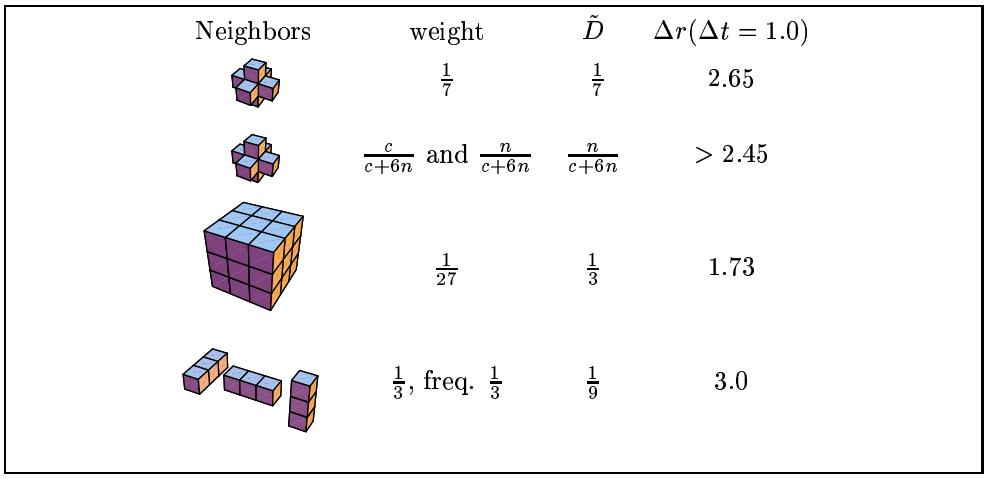

Figure 1: Diffusion operators.

If Δt is too big, this approximation can be very bad. One solution is to calculate the exact solution to Eq. (6):

$$x(t + \Delta t) = x(t) + \int_t^{t+\Delta t} f(x(\tau))d\tau. \tag{8}$$

This integration can be done analytically or using high-order numerical integration methods. Taking spatial dependence back into account, in the updating we replace Eq. (4b) by

$$\hat{x}(t, r) = \tfrac{1}{c}\tilde{x}(t, \mathbf{r}) \tag{9a}$$

$$\hat{x}(t + \Delta t, \mathbf{r}) = \hat{x}(t, \mathbf{r}) + \int_t^{t+\Delta t} f\left(\hat{x}(\tau, \mathbf{r})\right)\, d\tau \tag{9b}$$

$$\tilde{\hat{x}}(t, \mathbf{r}) = \tfrac{1}{c}\Big(\tilde{x}(t, \mathbf{r}) + c\Big[\hat{x}(t + \Delta t, r) - \hat{x}(t, r)\Big]\Big). \tag{9c}$$

It is important to note that Equations (9a) and (9b) are only used to construct the lookup table, i.e., the integration is done only once for each possible input value during the initialization phase. The final simulation uses exactly the same procedure as before, and runs exactly at the same speed. The advantage is that we have eliminated the error coming from the Euler approximation Eq. (7) and thus we can use larger Δt. Note that the approximation of the diffusion term is only exact to $O(\Delta t)$, so that the interaction of diffusion and reaction still limits the time step.

4 Examples

As an example, we show travelling waves in the FitzHugh-Nagumo model Eqns. (2) in one, two, and three dimensional simulations. The size of the simulations is 100 cells in 1-D, 100^2 cells in 2-D, and 150^3 in 3-D and results can be seen in Figure 2. The three-dimensional simulation needs more space because the phenomena are more complex.

The parameters of the CA model are as follows: Only one variable is involved in the diffusion operator, since the diffusion coefficient for the second variable is zero. The diffusion operator used is the three-step splitting method with only two neighbors in each step. The variables are discretized in 682 levels (u) and 511 levels

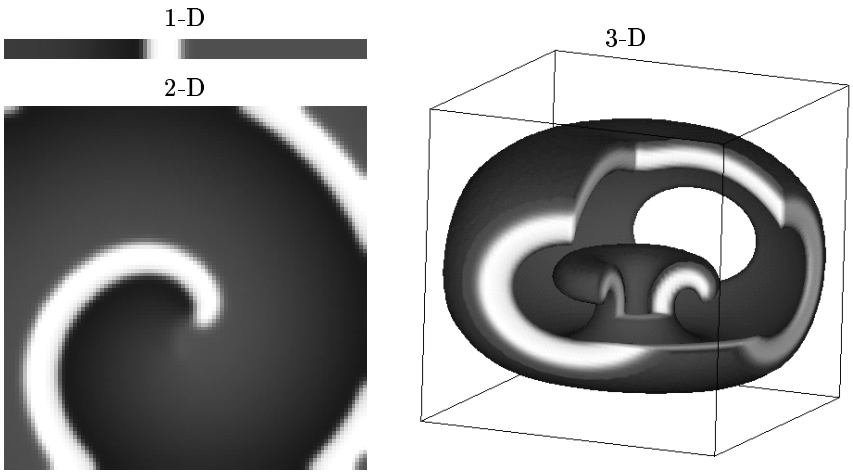

Figure 2: Wave in an excitable medium in one, two, and three dimensions.

(v). The rounding operator is deterministic and the time step is $\Delta t = 0.5$. This leads to $\Delta r = 2.12$ for $D = 1$. With these parameters, one full rotation of the scroll wave takes about 400 time steps.

In one dimension, travelling waves occur. In two dimensions these travelling waves can form rotating spiral waves when they are interrupted. In three dimensions, scroll rings are some of the simplest phenomena that are genuinely three-dimensional. In each case we show the simplest phenomenon that is not a direct extension of a lower-dimensional case.

The scroll wave in three dimensions can be thought of as a series of spiral waves stacked along a circle. The circle formed by the tip of the spirals is called the scroll filament. If the spirals are also rotated as they are stacked along the circle, we obtain a twisted scroll wave, as shown in Figure 3. Here the filament is shown with a series of small black dots. The topology of this twisted scroll ring requires that a second filament thread the circle. More complicated structures in three-dimensional excitable media are simulated in [3], using a somewhat different CA approach.

The second example is the model for the CIMA reaction, Eqns. (3). Two-dimensional simulations are reported in [12]. In this case the parameters of the CA model are as follows: Since the two variables have very different diffusion coefficients, we need two different operators. For the variable u with the smaller diffusion coefficient, we use the splitting method as before. For v with $D_v = 9D_u$, we use a cube of $5 \times 5 \times 5$ cells, which has $\tilde{D} = 1$. The calculation of the sum of all elements on the cube can be achieved using only 6 additions by a method of moving averages that carries over directly from the two-dimensional case [8, 12]. The variables are discretized in 250 levels (u) and 16 levels (v). For v, we use only 16 levels because the table for the complete updating function has $16 \times 5 \times 5 \times 5 = 2000$ entries for v, multiplied by the $250 * 3 = 750$ entries for u.

The rounding operator is probabilistic and the time step is $\Delta t = 0.03$. With these parameters, the apperance of patterns from uniform initial conditions takes about 10000 time steps. Resulting patterns are shown in Figure 4.

5 Conclusion

We have presented an extension of a class of cellular automata for reaction-diffusion systems to three dimensions. The basic ideas for these automata can be carried over

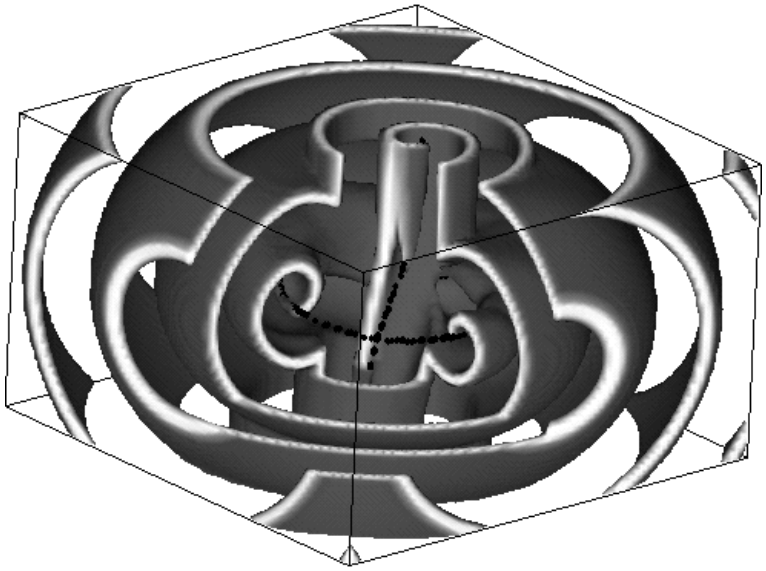

Figure 3: Three-dimensional twisted scroll wave in an excitable medium. The scroll ring surrounds another vertical filament (line of spiral tips) by topological necessity.

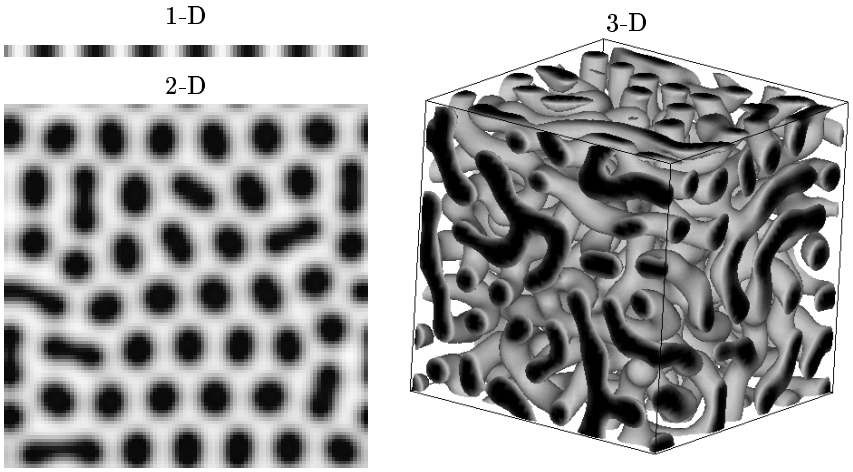

Figure 4: Patterns of the CIMA model in one, two, and three dimensions.

from two-dimensional models. Diffusion is realized through a local averageing, and all the nonlinear reaction terms are collected in a table-lookup. The need to increase time- and space scales led to the development of smaller neighborhoods for the diffusion operator, and to the possibility of increasing the time step by introducing exact integration over a time period Δt instead of using the Euler-approximation. The combination of these improvents makes large three-dimensional simulations possible. We have presented examples of such simulations of excitable media and of a pattern-forming chemical reaction.

References

[1] P. de Kepper, V. Castets, E. Dulos, and J. Boissonade. Turing-type chemical patterns in the chlorite-iodide-malonic acid reaction. *Physica D*, 49:161–169, 1991.

[2] R. FitzHugh. Impulse and physiological states in models of nerve membrane. *Biophysics J.*, 1:445–466, 1961.

[3] Chris Henze and John J. Tyson. Cellular automaton model of three-dimensional excitable media. *J. Chem. Soc., Faraday Trans.*, 92(16):2883–2895, 1996.

[4] Raymond Kapral. Chemical waves and coupled map lattices. In K. Kaneko, editor, *Theory and Applications of Coupled Map Lattices*, pages 135–168. Wiley, 1993.

[5] Istvàn Lengyel and Irving R. Epstein. Modeling of Turing structures in the chlorite-iodide-malonic acid-starch reaction system. *Science*, 251:650–652, 1991.

[6] J. S. Nagumo, S. Arimoto, and S. Yoshizawa. An active pulse transmission line simulating nerve axon. *Proc. IRE*, 50:2061–2071, 1962.

[7] Q. Ouyang and Harry L. Swinney. Transition from a uniform state to hexagonal and striped Turing patterns. *Nature*, 352:610–612, 1991.

[8] Jörg R. Weimar. *Cellular Automata for Reactive Systems.* PhD thesis, Université Libre de Bruxelles, Belgium, 1995.

[9] Jörg R. Weimar. Cellular automata for reaction-diffusion systems. *Parallel Computing*, 23(11):1699–1715, 1997.

[10] Jörg R. Weimar. *Simulation with Cellular Automata.* Logos-Verlag, Berlin, 1998.

[11] Jörg R. Weimar and Jean-Pierre Boon. Class of cellular automata for reaction-diffusion systems. *Physical Review E*, 49(2):1749–1752, 1994.

[12] Jörg R. Weimar and Jean-Pierre Boon. New class of cellular automata for reaction-diffusion systems applied to the CIMA reaction. In A. Lawniczak and R. Kapral, editors, *Lattice Gas Automata and Pattern Formation*, volume 6, pages 239–247, Waterloo, Ont, Canada, 1996. Fields Institute.

[13] A. T. Winfree. *Vortex re-entry in healthy myocardium*, pages 609–625. Academic Press Ltd., 1989.

[14] Arthur T. Winfree. *When time breaks down.* Princeton University Press, Princeton, NJ, 1987.